Gradient recovery for elliptic interface problem: I. body-fitted mesh

Hailong Guo[1,*], and Xu Yang[1]

[1] *Department of Mathematics, University of California Santa Barbara, CA, 93106, USA*

Abstract. In this paper, we propose a new gradient recovery method for elliptic interface problem using body-fitted mesh. Due to the lack of regularity of the solution at the interface, standard gradient recovery methods fail to give superconvergent results, and thus will lead to overrefinement when served as *a posteriori* error estimator. This drawback is overcome by designing a new gradient recovery operator. We prove the superconvergence of the new method for both mildly unstructured mesh and adaptive mesh and present several numerical examples to verify the superconvergence and its robustness as *a posteriori* error estimator.

AMS subject classifications: 65L10, 65L60, 65L70

Key words: elliptic interface problem, gradient recovery, superconvergence, body-fitted mesh, *a posteriori* error estimator, adaptive method.

1 Introduction

Interface problem frequently appears in the fields of fluid dynamics and material science, where the background consists of rather different materials. The numerical challenge comes from discontinuities of the coefficient at the interface, where the solution is not smooth in general. Computational methods for elliptic interface problem have been studied intensively in literature, which can be roughly categorized into two types: unfitted mesh methods and body-fitted mesh methods.

Numerical methods based on unfitted mesh solve interface problems on Cartesian grids, among which, famous examples include immersed boundary method (IBM) by Peskin [35, 36] and immersed interface method (IIM) by Leveque and Li [24], just to name a few. We refer interested readers to [26] for a review of the literature. IBM uses Dirac δ-function to model discontinuity and discretizes it to distribute a singular source to the nearest grid point. IIM constructs a special finite difference scheme near the interface to get an accurate approximation of the solution. It was further developed in the framework

*Corresponding author. *Email addresses:* hlguo@math.ucsb.edu (H. Guo), xuyang@math.ucsb.edu (X. Yang)

of finite element method [25, 27, 28], which modifies basis functions on interface elements. Moreover, in [20,21], a special weak form was derived based on the Petrov-Galerkin method to discretize elliptic interface problem. A shortcoming of unfitted mesh methods is that the resulting discretized linear system is in general non-symmetric and indefinite even though the original continuous problem is self-adjoint.

Body-fitted mesh methods require mesh grids to align with the interface in order to capture discontinuity. The resulting discretized linear system is symmetric and positive definite if the original continuous problem is self-adjoint. Error estimates for finite element method with body-fitted mesh have been established by [2, 6, 12, 42]. In particular, [12] showed that smooth interface can be approximated by linear interpolation of distinguished points on the interface. Although the solution to interface problem has low global regularity, the finite element approximation was shown to have nearly the same optimal error estimates in both L^2 and energy norms as for regular (non-interface) problems.

Meanwhile, superconvergence analysis has attracted considerable attention in the community of finite element method, and theories have been well developed for regular problems [3, 9, 39, 47]. Then it is natural to ask if one can obtain similar superconvergence results for elliptic interface problem. However, limited work has been done in this direction due to the lack of regularity of solution at the interface. Recently, [13, 14] proposed two special interpolation formulae to recover flux for one-dimensional linear and quadratic immersed finite element methods. Supercloseness was established between finite element solution and linear interpolation of the true solution in [40].

In this paper, we aim to develop a gradient recovery technique for elliptic interface problem based on body-fitted finite element discretization. Standard gradient recovery operators, including superconvergent patch recovery (SPR) [48, 49] and polynomial preserving recovery (PPR) [32,33,44], produce superconvergent recovered gradient only when the solution is smooth enough. Therefore, they can not be applied directly to elliptic interface problem since the solution has low regularity at the interface due to the discontinuity of coefficients. Furthermore, building up a recovery-type *a posteriori* error estimator based on these methods will lead to overrefinement as studied in [8].

An observation that we rely on is that, even though the solution has low global regularity, it is in general piecewise smooth on each subdomain separated by the smooth interface (special case as Kellogg problem will be also discussed in Example 5.4). This motivates us to develop a new gradient recovery method by applying PPR gradient operator on each subdomain since PPR is a local gradient recovery method. One one hand, for a node away from the interface, we use stand PPR gradient recovery operator; On the other hand, for a node close to the interface, we design the gradient recovery operator by fitting a quadratic polynomial in the least-squares sense only using the sampling points in each subdomain. This will generate two approximations of the gradient in each subdomain for a node on the interface, which is consistent with the fact that the solution, in general, is not continuously differentiable at the interface. The method is to use a divide-and-conquer strategy, which has also been used in the immersed finite element method [25, 27, 28].

We prove that the proposed gradient recovery method has superconvergence for the

following two types of meshes: Benefited from [40] on the approximation estimate and supercloseness, we are able to establish the superconvergence theory on mildly unstructured meshes; Using the practical assumption and supercloseness result in [41] for adaptive mesh, we show that the proposed recovered gradient method is superconvergent to exact gradient on adaptive mesh. Therefore, the method provides an asymptotically exact *a posteriori* error estimator for elliptic interface problem. Compared to the *a posteriori* error estimator in [4, 11, 30] and recovery-type error estimator in [8], the estimator based on the proposed gradient recovery is easier in implementation and asymptotically more exact, which will be verified by two-dimensional numerical examples.

The rest of the paper is organized as follows. In Section 2, we introduce elliptic interface problem and its finite element approximation based on the body-fitted mesh. In Section 3, we first give a brief introduction to polynomial preserving recovery method, based on which, we develop a new gradient recovery method for elliptic interface problem. In Section 4, superconvergence is proved for the proposed gradient recovery operator on both mildly unstructured mesh and adaptively refined mesh. In addition, we show that the method provides an asymptotically exact *a posteriori* error estimator for elliptic interface problem. In Section 5, several numerical examples are presented to confirm our theoretical results. Conclusive remarks are made in Section 6.

2 Finite element method for elliptic interface problem

In this section, we first introduce elliptic interface problem and then describe the finite element approximation using a body-fitted mesh.

2.1 Elliptic interface problem

Let Ω be a bounded polygonal domain with Lipschitz boundary $\partial\Omega$ in $\mathbb{R}^2$. A C^2-curve Γ divides Ω into two disjoint subdomains Ω^- and Ω^+, which is typically characterized by zero level set of some level set function ϕ [34, 38]. Then $\Omega^-=\{z\in\Omega|\phi(z)<0\}$ and $\Omega^+=\{z\in\Omega|\phi(z)>0\}$. We shall consider the following elliptic interface problem

$$-\nabla\cdot(\beta(z)\nabla u(z))=f(z),\quad z \text{ in } \Omega\backslash\Gamma, \tag{2.1}$$

$$u=0,\qquad z \text{ on } \partial\Omega, \tag{2.2}$$

where the diffusion coefficient $\beta(z)\geq\beta_0$ is a piecewise smooth function, i.e.

$$\beta(z)=\begin{cases}\beta^-(z) & \text{if } z\in\Omega^-,\\ \beta^+(z) & \text{if } z\in\Omega^+,\end{cases} \tag{2.3}$$

which has a finite jump of function values across the interface Γ. At the interface Γ, one has the following jump conditions

$$[u]_\Gamma=u^+-u^-=0, \tag{2.4}$$

$$[\beta u_n]_\Gamma=\beta^+u_n^+-\beta^-u_n^-=g, \tag{2.5}$$

where u_n denotes the normal flux $\nabla u\cdot n$ with n being the unit outer normal vector of the interface Γ.

Notations. Let C denote a generic positive constant which may be different at different occurrences. For the sake of simplicity, we use $x\lesssim y$ to mean that $x\leq Cy$ for some constant C, which is independent of mesh size and the interface location but may depend on the coefficient β.

Standard notations for Sobolev spaces and their associate norms given in [7,15,18] are adopted in this paper. Moreover, for a subdomain A of Ω, let $\mathbb{P}_m(A)$ be the space of polynomials of degree less than or equal to m in A and n_m be the dimension of $\mathbb{P}_m(A)$ which equals to $\frac{1}{2}(m+1)(m+2)$. $W^{k,p}(A)$ denotes the Sobolev space with norm $\|\cdot\|_{k,p,A}$ and seminorm $|\cdot|_{k,p,A}$. When $p=2$, $W^{k,2}(A)$ is simply denoted by $H^k(A)$ and the subscript p is omitted in its associate norm and seminorm. As in [40], denote $W^{k,p}(\Omega^-\cup\Omega^+)$ as the function space consisting of piecewise Sobolev function w such that $w|_{\Omega^-}\in W^{k,p}(\Omega^-)$ and $w|_{\Omega^+}\in W^{k,p}(\Omega^+)$. For the function space $W^{k,p}(\Omega^-\cup\Omega^+)$, define norm as

$$\|w\|_{k,p,\Omega^-\cup\Omega^+}=\left(\|w\|^p_{k,p,\Omega^-}+\|w\|_{k,p,\Omega^+}\right)^{1/p},$$

and seminorm as

$$|w|_{k,p,\Omega^-\cup\Omega^+}=\left(|w|^p_{k,p,\Omega^-}+|w|_{k,p,\Omega^+}\right)^{1/p}.$$

The variational formulation of the elliptic interface problem (2.1)–(2.5) is given by finding $u\in H^1_0(\Omega)$ such that

$$(\beta\nabla u,\nabla v)=(f,v)-\langle g,v\rangle,\quad \forall v\in H^1_0(\Omega), \tag{2.6}$$

where $(\cdot,\cdot)$ and $\langle\cdot,\cdot\rangle$ are standard L_2-inner product in the spaces $L^2(\Omega)$ and $L^2(\Gamma)$ respectively. By the positiveness of β, Lax-Milgram Theorem implies (2.6) has a unique solution. It is proved in [12,37] that $u\in H^r(\Omega^-\cup\Omega^+)$ for $0\leq r\leq 2$ and

$$\|u\|_{r,\Omega^-\cup\Omega^+}\lesssim\|f\|_{0,\Omega}+\|g\|_{r-3/2,\Gamma}, \tag{2.7}$$

provided that $f\in L^2(\Omega)$ and $g\in H^{r-3/2}(\Gamma)$.

Remark 2.1. For the sake of easing theoretical analysis, we simply assume homogeneous jump of function value. In fact, one can extend the method to inhomogeneous jump of function value $[u]_\Gamma=q$ by defining a piecewise smooth function $\hat{q}$ that satisfies $\hat{q}|_\Gamma=q$ and $\hat{q}|_{\partial\Omega}=0$, and then the problem (2.1)–(2.5) is equivalent to find $u=w+\hat{q}$ with $w\in H^1_0(\Omega)$ such that

$$(\beta\nabla w,\nabla v)=(f,v)-\langle g,v\rangle-(\beta\nabla\hat{q},\nabla v),\quad \forall v\in H^1_0(\Omega).$$

2.2 Finite element approximation

Let $\mathcal{T}_h$ be a body-fitted triangulation of Ω. Then every triangle $T\in\mathcal{T}_h$ belongs to one of the following three different cases:

(a) $T\subset\overline{\Omega^-}$;

(b) $T\subset\overline{\Omega^+}$;

(c) $T\cap\Omega^-\neq\emptyset$ and $T\cap\Omega^+\neq\emptyset$; in that case, two of vertices of T lie on Γ.

For any $T\in\mathcal{T}_h$, denote its diameter and supremum of the diameters of the circles inscribed in T by h_T and ρ_T respectively. Let $h=\max_{T\in\mathcal{T}_h}h_T$. Assume that the triangulation of Ω is shape-regular in the sense that there is a constant ξ such that $\frac{h_T}{\rho_T}\leq\xi$ for all $T\in\mathcal{T}_h$. Denote Γ_h as an approximation to Γ which consists of the edges with both endpoints lying on Γ. The domain Ω is divided into two parts Ω_h^- and Ω_h^+ by Γ_h, which are the approximations of Ω^- and Ω^+ respectively.

The element in $\mathcal{T}_h$ can be categorized into two types: regular elements and interface elements. An element T is called an interface element if it has exactly two vertices on Γ; otherwise, it is called regular element. The set of all interface elements is denoted by $\mathcal{T}_h^*$. For each element $T\in\mathcal{T}_h^*$, let $T^-=T\cap\Omega^-$ and $T^+=T\cap\Omega^+$. Since Γ is C^2, one has

$$|T^-|\lesssim h_T^3,\text{ or }|T^+|\lesssim h_T^3,$$

as shown in [12].

For each edge e on Γ_h, define a projection $\mathcal{P}_h$ [6,40] from e to Γ as

$$\mathcal{P}_h(z)=z+d(z)n_h,\quad\forall z\in e,\tag{2.8}$$

where n_h is the unit normal vector of e pointing from Ω^- to Ω^+ and $d(z)$ is the sign distance function between z and Γ along n_h. Note that $\mathcal{P}_h$ is a point in Γ for each $z\in e$. According to [6,40], the projection $\mathcal{P}_h$ and its inverse are well defined when the length of e is small enough.

Let V_h be the continuous linear finite element space and $V_{h,0}=V_h\cap H_0^1(\Omega)$. We approximate the diffusion coefficient β by β_h with $\beta_h|_T=\beta^-$ if $T\in\Omega_h^-$ and $\beta_h|_T=\beta^+$ if $T\in\Omega_h^+$. Then the linear finite element approximation of the variational problem (2.6) is to find $u_h\in V_{h,0}$ such that

$$(\beta_h\nabla u_h,\nabla v_h)=(f,v_h)-\langle g_h,v_h\rangle_{\Gamma_h},\quad\forall v_h\in V_{h,0},\tag{2.9}$$

where $g_h=g(P_h(z))$ and $\langle\cdot,\cdot\rangle_{\Gamma_h}$ is L^2-inner product of $L^2(\Gamma_h)$. Moreover, [12,42,45] proved the following convergence results for the finite element approximation (2.9).

Theorem 2.2. *Let u and u_h be the solution to* (2.6) *and* (2.9) *respectively. If $u\in H^2(\Omega^-\cup\Omega^+)$ and $g\in H^2(\Gamma)$, then we have*

$$\|\nabla u-\nabla u_h\|_{0,\Omega}\lesssim h|\log h|^{1/2}(\|f\|_{0,\Omega}+\|g\|_{2,\Gamma}),\tag{2.10}$$

$$\|u-u_h\|_{0,\Omega}\lesssim h^2|\log h|^{1/2}(\|f\|_{0,\Omega}+\|g\|_{2,\Gamma}).\tag{2.11}$$

Note that the error estimate (2.10) is nearly optimal due to the existence of $|\log h|^{1/2}$.

3 Gradient recovery for elliptic interface problem

In this section, we first summarize the polynomial preserving recovery(PPR) method proposed by Zhang and Naga in [32, 33, 44] for finite element approximation of standard elliptic problem, then based on which, we propose a new gradient recovery method for elliptic interface problem.

3.1 Polynomial preserving recovery

For any vertex z and $n\in\mathbb{Z}^+$, let $\mathcal{L}(z,n)$ denote the union of elements in the first n layers around z, i.e.,

$$\mathcal{L}(z,n):=\bigcup\{T:T\in\mathcal{T}_h,T\cap\mathcal{L}(z,n-1)\neq\emptyset\}, \tag{3.1}$$

where $\mathcal{L}(z,0):=\{z\}$.

The set of all mesh vertices and edges are denoted by $\mathcal{N}_h$ and $\mathcal{E}_h$ respectively. The standard Lagrange basis of V_h is denoted by $\{\phi_z:z\in\mathcal{N}_h\}$ with $\phi_z(z')=\delta_{zz'}$ for all $z,z'\in\mathcal{N}_h$. Let us introduce the PPR gradient recovery operator $G_h:V_h\to V_h\times V_h$. For any vertex z, let $\mathcal{K}_z$ be a patch of elements around z. Select all nodes in $\mathcal{N}_h\cap\mathcal{K}_z$ as sampling points and fit a polynomial $p_z\in\mathbb{P}_2(\mathcal{K}_z)$ in the least-squares sense at those sampling points, i.e.

$$p_z=\arg\min_{p\in\mathbb{P}_2(\mathcal{K}_z)}\sum_{\tilde{z}\in\mathcal{N}_h\cap\mathcal{K}_z}(u_h-p)^2(\tilde{z}). \tag{3.2}$$

Then the recovered gradient at z is defined as

$$(G_hu_h)(z)=\nabla p_z(z).$$

After obtaining recovered gradient value at all nodal points, we define the recovered gradient G_h on the whole domain by

$$G_hu_h:=\sum_{z\in\mathcal{N}_h}(G_hu_h)(z)\phi_z. \tag{3.3}$$

Remark 3.1. If u_h is a function in V_h, then ∇u_h is a piecewise constant function and hence is discontinuous on Ω. However, the recovered gradient G_hu_h is a continuous piecewise linear function. In that sense, G_h can be viewed as a smoothing operator to smooth a discontinuous piecewise constant function into a continuous piecewise linear function.

To complete the definition of PPR, we need to define $\mathcal{K}_z$. If z is an interior vertex, $\mathcal{K}_z$ is defined as the smallest $\mathcal{L}(z,n)$ that guarantees the uniqueness of p_z in (3.2) [32,33,44]. In the case that $z\in\mathcal{N}_h\cup\partial\Omega$, let n_0 be the smallest positive integer such that $\mathcal{L}(z,n_0)$ has at least one interior mesh vertex. Then, we define

$$\mathcal{K}_z=\mathcal{L}(z,n_0)\cup\{\mathcal{K}_{\tilde{z}}:\tilde{z}\in\mathcal{L}(z,n_0)\text{ and }\tilde{z}\text{ an interior vertex}\}.$$

Remark 3.2. In order to avoid numerical instability, all discrete least-squares fittings are carried out on a reference patch ω_z.

The PPR gradient recovery operator G_h has the followings properties, as proved in [19, 32, 33, 44]:

I. G_h is a linear operator.

II. G_h preserves quadratic polynomials. Consequently, G_h enjoys the approximation property
$$\|\nabla u - G_h u_I\|_{0,\Omega} \lesssim h^2 |u|_{3,\Omega}, \quad \forall u \in H^3(\Omega), \tag{3.4}$$
where u_I is the linear interpolation of u in V_h.

III. $\|G_h v_h\|_{0,\Omega} \lesssim \|\nabla v_h\|_{0,\Omega}, \forall v_h \in V_h$.

3.2 Improved polynomial preserving recovery operator

As we mentioned in Remark 3.1, standard PPR can be viewed a smoothing operator. However, ∇u is discontinuous across the interface Γ for the elliptic interface problem, and thus standard PPR won't work since it provides continuous gradient approximation. Noticing that in many cases, even though u have low global regularity due to the existence of the interface, $u|_{\Omega^-}$ (or $u|_{\Omega^+}$) is smooth, which motivates us to recover a piecewise continuous gradient approximation instead.

Let Ω_h be the body-fitted triangulation introduced in Subsection 2.2. The approximate interface Γ_h divides the triangulation Ω_h into two disjoint sets:

$$\mathcal{T}_h^- := \left\{ T \in \mathcal{T}_h | \text{ all three vertices of } T \text{ are in } \overline{\Omega^-} \right\}, \tag{3.5}$$
$$\mathcal{T}_h^+ := \left\{ T \in \mathcal{T}_h | \text{ all three vertices of } T \text{ are in } \overline{\Omega^+} \right\}. \tag{3.6}$$

Let V_h^- and V_h^+ be the continuous linear finite element spaces defined on $\mathcal{T}_h^-$ and $\mathcal{T}_h^+$ respectively.

Denote the PPR gradient recovery operator on V_h^- by G_h^-. Then G_h^- is a linear bounded operator from V_h^- to $V_h^- \times V_h^-$. Similarly, let G_h^+ be PPR gradient recovery operator from V_h^+ to $V_h^+ \times V_h^+$. Then, for any $u_h \in V_h$, we define the global gradient recovery operator $G_h^I : V_h \to (V_h^- \cup V_h^+) \times (V_h^- \cup V_h^+)$ as

$$(G_h^I u_h)(z) = \begin{cases} (G_h^- u_h)(z) & \text{if } z \in \overline{\Omega_h^-}, \\ (G_h^+ u_h)(z) & \text{if } z \in \overline{\Omega_h^+}. \end{cases} \tag{3.7}$$

Specifically, we define $(G_h^I u_h)(z)$ according to the location of z:

Case 1. If z is far from the approximate interface Γ_h, $(G_h^I u_h)(z)$ is the standard PPR recovered gradient at z.

Case 2. If z is close to the approximate interface Γ_h, $(G_h^I u_h)(z)$ is given by fitting a quadratic polynomial in the least-squares sense using sampling points only from $\mathcal{T}_h^-$ or only from $\mathcal{T}_h^+$.

Case 3. If z is on approximate interface Γ_h, $(G_h^I u_h)(z)$ is given two values: one by $(G_h^- u_h)(z)$ and the other by $(G_h^+ u_h)(z)$.

We call G_h^I as improved polynomial preserving recovery (IPPR) operator.

Remark 3.3. Given a function u_h in V_h, $G_h^I u_h$ is not a function in $V_h \times V_h$, since it is two-valued on the approximate interface Γ_h as described in Case 3.

Remark 3.4. The choice of G_h^I is not limited to PPR gradient recovery operator, and in fact, it can be any local gradient recovery operator such as weighted averaging gradient recovery operator [1] and SPR gradient recovery operator [48, 49]. One can even use different gradient recovery operators on two subdomains separated by Γ_h, for example, PPR gradient recovery operator on V_h^- and SPR gradient recovery operator on V_h^+. We shall use PPR gradient recovery operator in this paper for convenience.

Remark 3.5. The IPPR operator can be generalized to the case when the domain Ω is divided into serval subdomains by defining the gradient recovery operator piecewise in each subdomain.

Moreover, we have the following approximation estimate for the IPPR gradient recovery operator G_h^I.

Theorem 3.6. *Let $G_h^I: V_h \to (V_h^- \cup V_h^+) \times (V_h^- \cup V_h^+)$ be the IPPR gradient recovery operator. Given $u \in H^3(\Omega^- \cup \Omega^+)$, then*

$$\|G_h^I u_I - \nabla u\|_{0,\Omega} \lesssim h^2 \|u\|_{3,\Omega^- \cup \Omega^+}, \tag{3.8}$$

where u_I is interpolation of u into linear finite element space V_h.

Proof. Notice that G_h^- and G_h^+ are the standard PPR gradient recovery operators. Formula (3.4) implies that

$$\|G_h^- u_I - \nabla u\|_{0,\Omega_h^-} \lesssim h^2 \|u\|_{3,\Omega^-}, \text{ and } \|G_h^+ u_I - \nabla u\|_{0,\Omega_h^+} \lesssim h^2 \|u\|_{3,\Omega^+}.$$

Therefore,

$$\begin{aligned} \|G_h^I u_I - \nabla u\|_{0,\Omega}^2 &= \|G_h^- u_I - \nabla u\|_{0,\Omega_h^-}^2 + \|G_h^+ u_I - \nabla u\|_{0,\Omega_h^+}^2 \\ &\lesssim h^4 \|u\|_{3,\Omega^-}^2 + h^4 \|u\|_{3,\Omega^+}^2 \\ &\lesssim h^4 \|u\|_{3,\Omega^- \cup \Omega^+}. \end{aligned}$$

□

4 Superconvergence Analysis

In this section, we prove that the IPPR gradient recovery method has superconvergence for both mildly unstructured mesh and adaptive mesh.

4.1 Superconvergence on mildly unstructured mesh

We first introduce the definition of the mesh structure which guarantees the supercloseness result.

Definition 4.1. 1. Two adjacent triangles are called to form an $\mathcal{O}(h^{1+\alpha})$ approximate parallelogram if the lengths of any two opposite edges differ only by $\mathcal{O}(h^{1+\alpha})$.

2. The triangulation $\mathcal{T}_h$ is called to satisfy Condition (σ,α) if there exist a partition $\mathcal{T}_{h,1}\cup\mathcal{T}_{h,2}$ of $\mathcal{T}_h$ and positive constants α and σ such that every two adjacent triangles in $\mathcal{T}_{h,1}$ form an $\mathcal{O}(h^{1+\alpha})$ parallelogram and

$$\sum_{T\in\mathcal{T}_{h,2}}|T|=\mathcal{O}(h^{\sigma}).$$

Under the above mesh condition, the following supercloseness result holds:

Theorem 4.1. *Let u be the solution to variational problem* (2.6) *and u_h be the finite element solution to* (2.9)*. If the body-fitted mesh satisfies Condition (σ,α) and $u\in H^3(\Omega^-\cup\Omega^+)\cap W^{2,\infty}(\Omega^-\cup\Omega^+)$, then for any $v_h\in V_{h,0}$, we have*

$$\begin{aligned}(\beta_h\nabla(u-u_I),\nabla v_h)\lesssim& h^{1+\rho}(\|u\|_{3,\Omega^-\cup\Omega^+}+\|u\|_{2,\infty,\Omega^-\cup\Omega^+})|v_h|_{1,\Omega}\\&+h^{\frac{3}{2}}\|u\|_{2,\infty,\Omega^-\cup\Omega^+}|v_h|_{1,\Omega},\end{aligned}\tag{4.1}$$

and

$$\begin{aligned}\|\nabla(u_I-u_h)\|_{0,\Omega}\lesssim& h^{1+\rho}(\|u\|_{3,\Omega^-\cup\Omega^+}+\|u\|_{2,\infty,\Omega^-\cup\Omega^+})\\&+h^{\frac{3}{2}}(\|u\|_{2,\infty,\Omega^-\cup\Omega^+}+\|g\|_{0,\infty,\Gamma}),\end{aligned}\tag{4.2}$$

where $\rho=\min(\alpha,\frac{\sigma}{2},\frac{1}{2})$ and $u_I\in V_h$ is the interpolation of u.

Proof. The proof is similar to the proof of Theorem 3.6 in [40] where we use the estimates in [43] instead of [10]. □

Remark 4.2. If $\Gamma=\Gamma_h$ or the flux jump g given by (2.5) vanishes with Γ smooth enough so that $|T^-|\lesssim h_T^4$ (or $|T^+|\lesssim h_T^4$), then one has the following $O(h^{1+\rho})$ improved supercloseness results

$$(\beta_h\nabla(u-u_I),\nabla v_h)\lesssim h^{1+\rho}(\|u\|_{3,\Omega^-\cup\Omega^+}+\|u\|_{2,\infty,\Omega^-\cup\Omega^+})|v_h|_{1,\Omega},\tag{4.3}$$

and

$$\|\nabla(u_I-u_h)\|_{0,\Omega}\lesssim h^{1+\rho}(\|u\|_{3,\Omega^-\cup\Omega^+}+\|u\|_{2,\infty,\Omega^-\cup\Omega^+}).\tag{4.4}$$

Remark 4.3. The difference between Theorem 4.1 and Theorem 3.6 in [40] lies in the condition of mesh structure. The $\mathcal{O}(h^{2\sigma})$ irregular mesh condition in [40] is just a special case of Condition (σ,α).

Remark 4.4. For the body-fitted mesh generated by Delaunay algorithm, the assumption that two adjacent triangles form $\mathcal{O}(h^{1+\alpha})$ approximate parallelogram is violated near boundary and interface, however, the summation of the area of such type triangles is bounded by $\mathcal{O}(h^{\sigma})$, and thus it satisfies Condition (σ,α).

The supercloseness result in Theorem 4.1 implies the following superconvergent result.

Theorem 4.5. *Under the same hypothesis as in Theorem 4.1, then we have*

$$\begin{aligned}\|\nabla u-G_h^I u_h\|_{0,\Omega}\lesssim & h^{1+\rho}(\|u\|_{3,\Omega^-\cup\Omega^+}+\|u\|_{2,\infty,\Omega^-\cup\Omega^+})+\\ & h^{\frac{3}{2}}(\|u\|_{2,\infty,\Omega^-\cup\Omega^+}+\|g\|_{0,\infty,\Gamma}),\end{aligned}\tag{4.5}$$

where $\rho=\min(\alpha,\frac{\sigma}{2},\frac{1}{2})$.

Proof. We decompose $\nabla u-G_h^I u_h$ as $(\nabla u-G_h^I u_I)-(G_h^I u_I-G_h^I u_h)$, and then by triangle inequality,

$$\begin{aligned}&\|\nabla u-G_h^I u_h\|_{0,\Omega}\\ \le&\|\nabla u-G_h^I u_I\|_{0,\Omega}+\|G_h^I u_I-G_h^I u_h\|_{0,\Omega}\\ \le&\|\nabla u-G_h^I u_I\|_{0,\Omega}+\|G_h^- u_I-G_h^- u_h\|_{0,\Omega_h^-}+\|G_h^+ u_I-G_h^+ u_h\|_{0,\Omega_h^+}\\ \le&\|\nabla u-G_h^I u_I\|_{0,\Omega}+\|\nabla(u_I-u_h))\|_{0,\Omega_h^-}+\|\nabla(u_I-u_h)\|_{0,\Omega_h^+}\\ \le&\|\nabla u-G_h^I u_I\|_{0,\Omega}+\|\nabla(u_I-u_h)\|_{0,\Omega},\end{aligned}\tag{4.6}$$

where we have used the boundedness property of PPR gradient recovery operator G_h^- and G_h^+. The first term can be bounded by Theorem 3.6 and the second term is estimated in Theorem 4.1, which completes the proof. □

Remark 4.6. Under the same assumptions in Remark 4.2, one has the following improved superconvergence result

$$\|\nabla u-G_h^I u_h\|_{0,\Omega}\lesssim h^{1+\rho}(\|u\|_{3,\Omega^-\cup\Omega^+}+\|u\|_{2,\infty,\Omega^-\cup\Omega^+}).\tag{4.7}$$

4.2 Superconvergence on adaptive mesh

In this subsection, for simplicity, we assume that the interface Γ does not cut through any element $T\in\mathcal{T}_h$, i.e. $\Gamma=\Gamma_h$, which implies $\Omega^-=\Omega_h^-$ and $\Omega^+=\Omega_h^+$. Furthermore, we assume that the solution u to (2.6) has a single singularity on the interface Γ, and without loss of generality, we assume that the singularity is at the origin and u^- (or u^+) can be decomposed into a smooth part w^- (or w^+) and singular part v^- (or v^+), i.e.,

$$u^-=w^-+v^-,\text{ and }u^+=w^++v^+,\tag{4.8}$$

where

$$\left|\frac{\partial^m w^-}{\partial x^i \partial y^{m-i}}\right| \lesssim 1, \text{ and } \left|\frac{\partial^m v^-}{\partial x^i \partial y^{m-i}}\right| \lesssim r^{\delta-m}, \tag{4.9}$$

and

$$\left|\frac{\partial^m w^+}{\partial x^i \partial y^{m-i}}\right| \lesssim 1, \text{ and } \left|\frac{\partial^m v^+}{\partial x^i \partial y^{m-i}}\right| \lesssim r^{\delta-m}, \tag{4.10}$$

with $r=\sqrt{x^2+y^2}$ and $0<\delta<2$ being a constant.

For any edge e of the mesh $\mathcal{T}_h$, let h_e be the length of the edge and r_e be the distance from the origin to the midpoint of e. If e is an interior edge, denote Ω_e to be the patch of e consisting of two triangles sharing the edge e. In addition, let $\underline{h} \simeq \min_{T\in\mathcal{T}_h} h_T$ and N be the number of vertices of $\mathcal{T}_h$. To get superconvergence, one also needs the following restriction on mesh structure.

Definition 4.2. The triangulation $\mathcal{T}_h$ is said to satisfy Condition (α,σ,μ) if there exist constants $\alpha>0$, $\sigma\geq 0$, and $\mu>0$ such that the interior edge can separated into two parts $\mathcal{E}_h=\mathcal{E}_{1,h}\oplus\mathcal{E}_{2,h}$: Ω_e forms an $\mathcal{O}\left(h_e^{1+\alpha}/r_e^{\alpha+\mu(1-\alpha)}\right)$ parallelogram for $\forall e\in\mathcal{E}_{1,h}$ and the number of edges in $\mathcal{E}_{2,h}$ satisfies $\#\mathcal{E}_{2,h}\lesssim N^\sigma$.

Note that the above mesh condition is a practical assumption for adaptive mesh as shown in [41]. In addition, we assume $h_T \simeq r_T^{1-\mu}\underline{h}^\mu$ for any $T\in\mathcal{T}_h$, and then we can establish the following supercloseness result on the adaptive mesh.

Theorem 4.7. *Let u be the solution to the variational problem* (2.6) *and u_h be the finite element solution to* (2.9)*. Suppose the adaptive refined mesh $\mathcal{T}_h$ satisfies Condition $(\alpha,\sigma,\delta/2)$, and $h_T \simeq r_T^{1-\delta/2}\underline{h}^{\delta/2}$ for any $T\in\mathcal{T}_h$. If u satisfied* (4.8)-(4.10)*, then for any $v_h\in V_{h,0}$, we have*

$$(\beta_h\nabla(u-u_I),\nabla v_h) \lesssim \frac{1+(\ln N)^{1/2}}{N^{1/2+\rho}}\|\nabla v_h\|_{0,\Omega}, \tag{4.11}$$

and

$$\|\beta_h^{1/2}(\nabla u_I-\nabla u_h)\|_{0,\Omega} \lesssim \frac{1+(\ln N)^{1/2}}{N^{1/2+\rho}}\|\nabla v_h\|_{0,\Omega}, \tag{4.12}$$

where $\rho=\min\left(\frac{\alpha}{2},\frac{1-\sigma}{2}\right)$ and u_I is the linear interpolation of u.

Proof. First, one can decompose $(\beta_h\nabla(u-u_I),\nabla v_h)$ as

$$\begin{aligned}
&(\beta_h\nabla(u-u_I),\nabla v_h)\\
=&(\beta_h^-(\nabla u^- - u_I^-),\nabla v_h)_{\Omega^-}+(\beta^+(\nabla u^+ - u_I^+),\nabla v_h)_{\Omega^+}\\
=&I_1+I_2.
\end{aligned}$$

Lemma 3.3 in [41] implies the following estimates for I_1 and I_2,

$$I_1 \lesssim \frac{1+(\ln N)^{1/2}}{N^{1/2+\rho}} \|\nabla v_h\|_{0,\Omega},$$
$$I_2 \lesssim \frac{1+(\ln N)^{1/2}}{N^{1/2+\rho}} \|\nabla v_h\|_{0,\Omega},$$

which completes the proof of (4.11). By (2.6) and (2.9), also noticing that $\Gamma = \Gamma_h$ and $\beta = \beta_h$, we have

$$(\beta_h \nabla(u_I - u_h), \nabla v_h) = (\beta_h \nabla(u_I - u), \nabla v_h).$$

Taking $v_h = u_I - u_h$ gives (4.12). □

Before presenting our main superconvergent theorem on the adaptively refined mesh, we need to estimate gradient recovery operator analogous to Theorem 3.6.

Theorem 4.8. *Under the same hypothesis as in Theorem 4.7. Then*

$$\|\nabla u - G_h^I u_I\|_{0,\Omega} \lesssim \frac{1+(\ln N)^{1/2}}{N}. \tag{4.13}$$

Proof. The definition of G_h^I produces

$$\|\nabla u - G_h^I u_I\|_{0,\Omega}^2 = \|\nabla u^- - G_h^- u_I^-\|_{0,\Omega^-}^2 + \|\nabla u^+ - G_h^+ u_I^+\|_{0,\Omega^+}^2. \tag{4.14}$$

Note that u^- (or u^+) has the decomposition (4.8) and G_h^- (or G_h^+) is the standard PPR gradient recovery operator. Lemma 5.2 in [41] implies

$$\|\nabla u^- - G_h^- u_I^-\|_{0,\Omega^-} \lesssim \frac{1+(\ln N)^{1/2}}{N}, \tag{4.15}$$
$$\|\nabla u^+ - G_h^+ u_I^+\|_{0,\Omega^+} \lesssim \frac{1+(\ln N)^{1/2}}{N}. \tag{4.16}$$

Combing (4.14)-(4.16) gives (4.13). □

Then we can prove the superconvergence as follows.

Theorem 4.9. *Under the same hypothesis as in Theorem 4.7. Then*

$$\|\beta^{1/2}(\nabla u - G_h^I u_h)\|_{0,\Omega} \lesssim \frac{1+(\ln N)^{1/2}}{N^{1/2+\rho}}, \tag{4.17}$$

where $\rho = \min\left(\frac{\alpha}{2}, \frac{1-\sigma}{2}\right)$.

Proof. The proof is essentially the same as in Theorem 4.5 where one should use Theorems 4.8 and 4.7 instead of Theorems 3.6 and 4.1. □

Using the IPPR gradient recovery operator G_h^I, one can define a local *a posteriori* error estimator on element $T\in\mathcal{T}_h$ as

$$\eta_T=\|\beta^{1/2}(G_h^I u_h-\nabla u_h)\|_{0,T}, \tag{4.18}$$

and the corresponding global error estimator as

$$\eta_h=\left(\sum_{T\in\mathcal{T}_h}\eta_T^2\right)^{1/2}. \tag{4.19}$$

Theorem 4.9 implies that η_h is asymptotically exact *a posteriori* error estimator for elliptic interface problem.

Theorem 4.10. *Under the same hypothesis as in Theorem 4.7. If*

$$\frac{1}{N^{1/2}}\lesssim\|\beta^{1/2}(\nabla(u-u_h))\|_{0,\Omega}, \tag{4.20}$$

then

$$\left|\frac{\eta_h}{\|\beta^{1/2}(\nabla u-\nabla u_h)\|_{0,\Omega}}-1\right|\lesssim\frac{1+(\ln N)^{1/2}}{N^{\rho}}, \tag{4.21}$$

where $\rho=\min\left(\frac{\alpha}{2},\frac{1-\sigma}{2}\right)$.

Remark 4.11. Assumption (4.20) is reasonable according to lower bounded estimates of approximation by finite element spaces [23, 29].

5 Numerical Examples

In this section, we present several numerical examples to illustrate the superconvergence of the IPPR gradient recovery method and confirm the theoretical results given in the previous section. We also make numerical comparisons to standard PPR method [32,33,44] to show the effectiveness. For convenience, we shall use the following error measurements in all examples:

$$De := \|u-u_h\|_{1,\Omega}, \qquad D^ie:=\|\nabla u_I-\nabla u_h\|_{0,\Omega}, \tag{5.1}$$

$$D^re := \|\nabla u-G_h^I u_h\|_{0,\Omega}, \quad D^pe:=\|\nabla u-G_h u_h\|_{0,\Omega}. \tag{5.2}$$

We would like to remark that all convergence rate will be computed in the degree of freedom (Dof), and since $\mathrm{Dof}\approx h^{-2}$ for a two-dimensional quasi-uniform mesh, the corresponding convergent rate in mesh size h is twice as much as what we present in the tables.

Example 5.1. In this example, we consider the elliptic interface problem (2.1) in the square domain $\Omega=(-1,1)\times(-1,1)$ with a circular interface of radius $r_0=0.5$ as studied in [28]. The exact solution is

$$u(z)=\begin{cases}\frac{r^3}{\beta^-} & \text{if } z\in\Omega_-,\\ \frac{r^3}{\beta^+}+\left(\frac{1}{\beta^-}-\frac{1}{\beta^+}\right)r_0^3 & \text{if } z\in\Omega^+,\end{cases}$$

where $r=\sqrt{x^2+y^2}$.

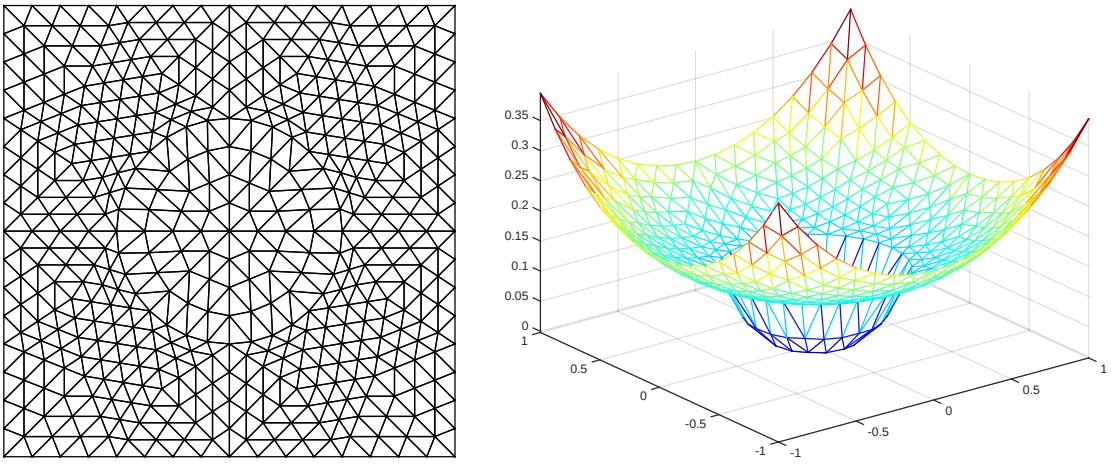

(a) (b)

Figure 1: Finite element mesh and solution for Example 5.1 with $\beta^+=10,\beta^-=1$: (a) Body-fitted mesh on the second level; (b) Finite element solution on the body-fitted mesh.

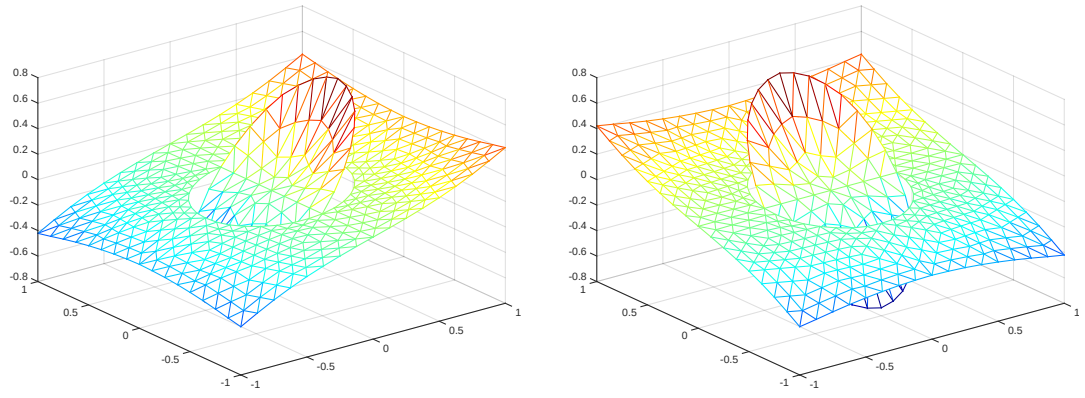

(a) (b)

Figure 2: Plot of recovered gradient for Example 5.1 with $\beta^+=10,\beta^-=1$: (a) x-component; (b) y-component.

Here we use five different levels of body-fitted meshes generated by a Delaunay mesh generator. Figure 1(a) plots the second level body-fitted mesh and Figure 1(b) plots the finite element solution on such a mesh. Figure 2 shows the recovered gradient.

Table 1: Numerical results for Example 5.1 with $\beta^+ = 10, \beta^- = 1$.

Dof	De	order	$D^i e$	order	$D^r e$	order	$D^p e$	order
129	1.35e-01	–	1.63e-02	–	1.34e-01	–	2.44e-01	–
481	7.25e-02	0.48	5.00e-03	0.90	2.30e-02	1.34	1.80e-01	0.23
1857	3.69e-02	0.50	1.40e-03	0.94	6.82e-03	0.90	1.30e-01	0.24
7297	1.85e-02	0.50	3.76e-04	0.96	1.84e-03	0.96	9.24e-02	0.25
28929	9.29e-03	0.50	9.81e-05	0.97	4.78e-04	0.98	6.52e-02	0.25

Table 2: Numerical results for Example 5.1 with $\beta^+ = 1000, \beta^- = 1$.

Dof	De	order	$D^i e$	order	$D^r e$	order	$D^p e$	order
129	1.25e-01	–	1.51e-02	–	1.47e-01	–	2.76e-01	–
481	6.76e-02	0.47	4.63e-03	0.90	2.29e-02	1.41	2.01e-01	0.24
1857	3.45e-02	0.50	1.29e-03	0.95	6.78e-03	0.90	1.45e-01	0.24
7297	1.73e-02	0.50	3.39e-04	0.98	1.83e-03	0.96	1.03e-01	0.25
28929	8.68e-03	0.50	8.70e-05	0.99	4.75e-04	0.98	7.24e-02	0.25

Table 3: Numerical results for Example 5.1 with $\beta^+ = 1000000, \beta^- = 1$.

Dof	De	order	$D^i e$	order	$D^r e$	order	$D^p e$	order
129	1.25e-01	–	1.51e-02	–	1.47e-01	0.00	2.76e-01	–
481	6.76e-02	0.47	4.63e-03	0.90	2.29e-02	1.41	2.01e-01	0.24
1857	3.45e-02	0.50	1.29e-03	0.95	6.78e-03	0.90	1.45e-01	0.24
7297	1.73e-02	0.50	3.39e-04	0.98	1.83e-03	0.96	1.03e-01	0.25
28929	8.68e-03	0.50	8.70e-05	0.99	4.75e-04	0.98	7.25e-02	0.25

Table 4: Numerical results for Example 5.1 with $\beta^+ = 1, \beta^- = 1000000$.

Dof	De	order	$D^i e$	order	$D^r e$	order	$D^p e$	order
129	5.27e-01	–	6.02e-02	–	1.84e-01	0.00	3.51e-01	–
481	2.64e-01	0.53	1.70e-02	0.96	3.06e-02	1.36	2.14e-01	0.38
1857	1.32e-01	0.51	4.66e-03	0.96	8.06e-03	0.99	1.48e-01	0.28
7297	6.60e-02	0.51	1.26e-03	0.96	2.10e-03	0.98	1.03e-01	0.26
28929	3.30e-02	0.50	3.37e-04	0.96	5.40e-04	0.98	7.25e-02	0.26

Tables 1-4 show the numerical results for four typical different jump ratios: $\beta^- / \beta^+ =$

1/10 (moderate jump), $\beta^-/\beta^+=1/1000$ (large jump), $\beta^-/\beta^+=1/1000000$ (huge jump), and $\beta^-/\beta^+=1000000$ (huge jump). In all different cases, optimal $\mathcal{O}(h)$ convergence can be observed for H^1-semi error of the finite element solution as given in Theorem 2.2. Notice that in this example, $g=0$ and Γ is arbitrary smooth. As discussed in Remark 4.2, one can have the supercloseness of $\mathcal{O}(h^2)$ as observed in Column 5 of Tables 1-4. We also notice that, for the convergence rate of recovered gradients, IPPR (D^re) superconverges at the order of $\mathcal{O}(h^2)$ while PPR (D^pe) converges suboptimally at the order of $\mathcal{O}(h^{0.5})$.

Example 5.2. In this example, we consider the flower-shape interface problem as studied in [31, 46]. The computational domain is $(-1,1)\times(-1,1)$. The interface curve Γ in polar coordinate is given by

$$r=\frac{1}{2}+\frac{\sin(5\theta)}{7},$$

which contains both convex and concave parts. The diffusion coefficient is piecewise constant with $\beta^-=1$ and $\beta^+=10$. The right hand function f in (2.1) is chosen to match the exact solution

$$u(z)=\begin{cases} e^{(x^2+y^2)}, & \text{if } z\in\Omega^+ \\ 0.1(x^2+y^2)^2-0.01\ln(2\sqrt{x^2+y^2}), & \text{if } z\in\Omega^+, \end{cases}$$

and the jump conditions at interface (2.4)-(2.5) are also provided by the exact solution.

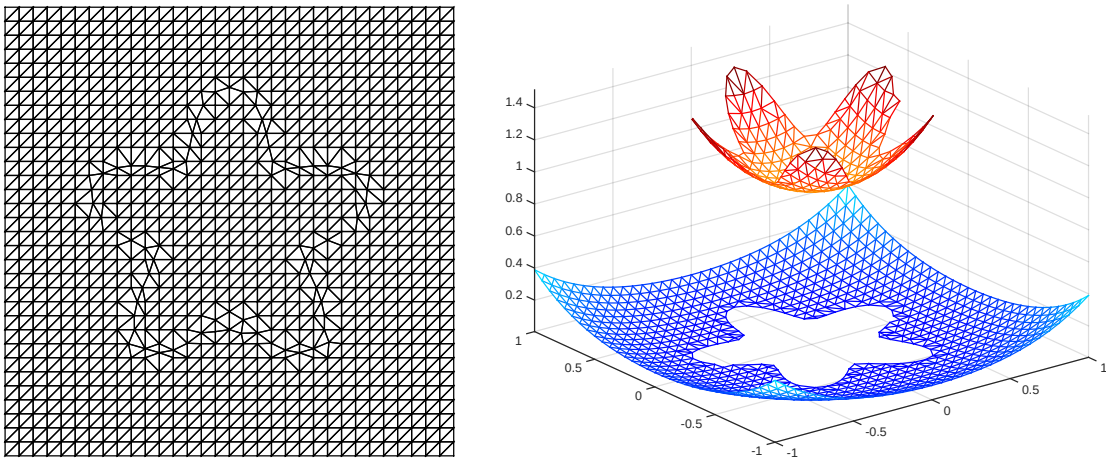

(a) (b)

Figure 3: Finite element mesh and solution for Example 5.2: (a) Body-fitted mesh on the first level; (b) Finite element solution on the body-fitted mesh.

We use Börgers algorithm [5] to generate the body-fitted meshes, with the first level of mesh shown in Figure 3(a) and the finite element solution in Figure 3(b). Figure 4 gives the plot of recovered gradient.

In Table 5, one can see that De decays at the rate of $\mathcal{O}(h)$ and D^ie superconverges at the rate of $\mathcal{O}(h^{1.5})$ which is consistent with Theorem 4.1. IPPR (D^re) has an $\mathcal{O}(h^{1.5})$

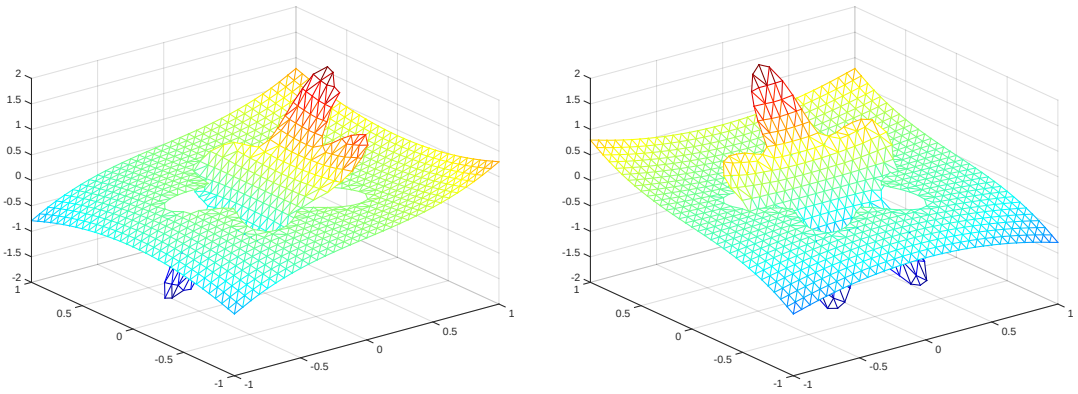

(a) (b)

Figure 4: Plot of recovered gradient for Example 5.2: (a) x-component; (b) y-component.

superconvergence that agrees with Theorem 4.5. However, no convergence is observed for standard PPR gradient recovery ($D^p e$) since the exact solution is only smooth on each subdomain.

Table 5: Convergence rate for Example 5.2.

Dof	De	order	$D^i e$	order	$D^r e$	order	$D^p e$	order
1089	7.25e-02	–	1.29e-02	–	1.15e-02	–	6.40e-01	–
4225	3.72e-02	0.49	4.67e-03	0.75	3.74e-03	0.83	6.35e-01	0.01
16641	1.87e-02	0.50	1.68e-03	0.74	1.19e-03	0.83	6.36e-01	-0.00
66049	9.42e-03	0.50	6.06e-04	0.74	3.75e-04	0.84	6.34e-01	0.00
263169	4.72e-03	0.50	2.18e-04	0.74	1.27e-04	0.78	6.34e-01	0.00
1050625	2.36e-03	0.50	7.69e-05	0.75	4.49e-05	0.75	6.33e-01	0.00

Example 5.3 This example is the same as the one used in [17]. We decompose the computational domain $\Omega=(-1,1)\times(-1,1)$ into two parts: $\Omega^-=\{z=(x,y)\in\Omega: x>0, y>0\}$ and $\Omega^+=\Omega\backslash\Omega^-$. The diffusion coefficient β in (2.1) is chosen as

$$\beta(z)=\begin{cases}\beta^- & \text{if } z\in\Omega^-,\\ 1 & \text{if } z\in\Omega^+,\end{cases}$$

with β^- being a constant. When $f=0$ in (2.1), the exact solution u in polar coordinate is given by

$$u(r,\theta)=\begin{cases} r^\mu\cos(\mu(\theta-\pi/4)) & \text{if } 0\le\theta\le\pi/2,\\ r^\mu\nu\cos(\mu(\theta-5\pi/4)) & \text{if } \pi/2\le\theta\le 2\pi,\end{cases}$$

where

$$\mu=\frac{4}{\pi}\left(\sqrt{\frac{3+\beta^-}{1+3\beta^-}}\right) \quad \text{and} \quad \nu=-\beta^-\frac{\sin(\mu\pi/4)}{\sin(3\mu\pi/4)}.$$

Note that $u \in H^{1+s}(\Omega^{\pm})$ for any $0 < s < \mu$.

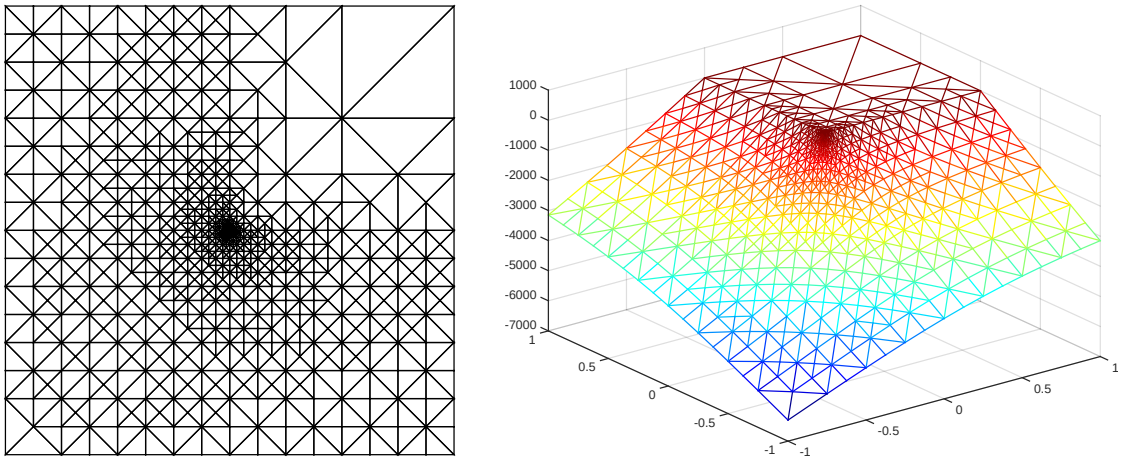

(a) (b)

Figure 5: Adaptive refined and solution of Example 5.3 with $\beta^- = 10000$. (a) Adaptive refined mesh. (b). Finite element solution on adaptive refined mesh h.

When $\beta^- > 1$, there is a singularity at the origin. To obtain optimal convergence rate, we use the adaptive finite element method based on the recovery-type *a posteriori* error estimator (4.18). In the numerical computation, we use the bulk marking strategy by [16] with $\theta = 0.2$, which marks a minimal set $\mathcal{M}_k \subset \mathcal{T}_k$ of elements in the following sense

$$\sum_{T \in \mathcal{M}_k} \eta_T^2 \geq \theta \sum_{T \in \mathcal{T}_k} \eta_T^2, \tag{5.3}$$

where k means the level of adaptive refinement. We start with a uniform initial mesh $\mathcal{T}_0$ consisting of 32 right triangles. Here, we only consider the cases when $\beta^- = 10, 100, 1000,$ and 10000. Figure 5(a) plots an adaptive refined mesh and 5(b) shows the finite element solution when $\beta^- = 10000$. It shows clearly that the refinement is concentrated on the singularity point.

Figures 6(a) and 6(b) give the numerical convergence rates for $\beta^- = 1000$ and $\beta^- = 10000$ respectively. In both cases, optimal convergence of $\mathcal{O}(N^{-0.5})$ for energy error and superconvergence rate of $\mathcal{O}(N^{0.95})$ can be observed, which is consistent with Theorem 4.9. We also plot the effective index

$$\kappa = \frac{\eta_h}{\|\beta^{1/2}(\nabla u - \nabla u_h)\|_{0,\Omega}}$$

in Figure 7. It shows the error indicator (4.18) is an asymptotically exact *a posteriori* error estimator for interface problem as in Theorem 4.10.

Example 5.4. In the example, we consider the Kellogg problem which is the benchmark problem of adaptive finite element method for interface problem studied by, for

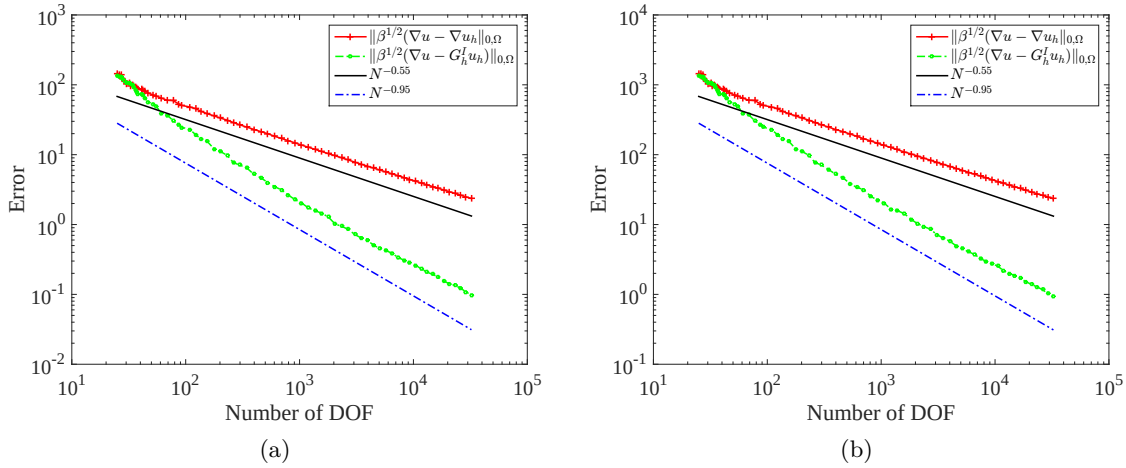

Figure 6: Convergence rates for Example 5.3: (a) $\beta^- = 1000$; (b) $\beta^- = 10000$.

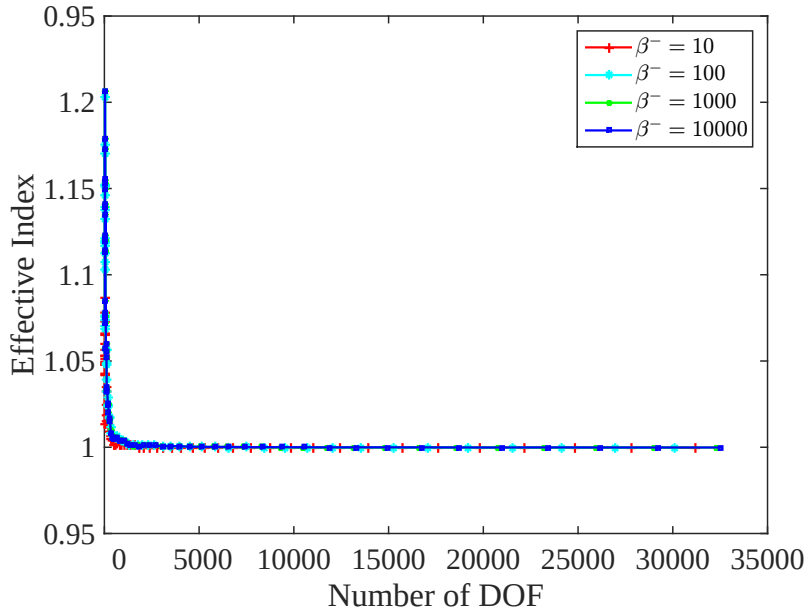

Figure 7: Graph of effective index of Example 5.3

example, [8, 11, 22, 30]. We choose the computational domain $\Omega = (-1,1)\times(-1,1)$, and consider (2.1) with $\beta(x) = R$ in the first and third quadrants and $\beta(x) = 1$ in the second and fourth quadrants. When $f = 0$ in (2.1), the exact solution u in polar coordinates is

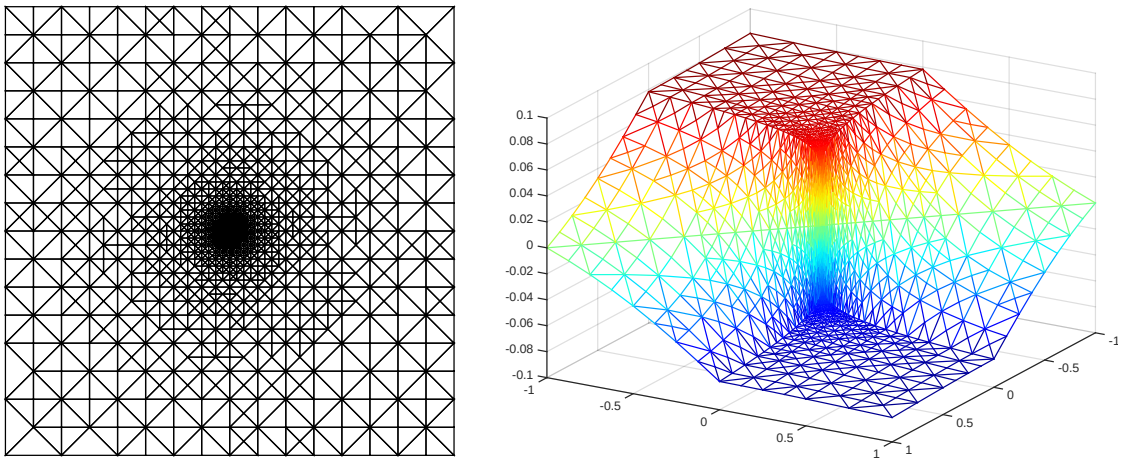

(a) (b)

Figure 8: Adaptive refined and solution of Example 5.3 with $\beta^-=10000$. (a) Adaptive refined mesh. (b). Finite element solution on adaptive refined mesh h.

given by $u(r,\theta)=r^\epsilon\mu(\theta)$ with

$$\mu(\theta)=\begin{cases}\cos((\pi/2-\xi)\epsilon)\cdot\cos((\theta-\pi/2+\nu)\epsilon) & \text{if } 0\le\theta\le\pi/2,\\ \cos(\nu\epsilon)\cdot\cos((\theta-\pi+\xi)\epsilon) & \text{if } \pi/2\le\theta\le\pi,\\ \cos(\xi\epsilon)\cdot\cos((\theta-\pi-\nu)\epsilon) & \text{if } \pi\le\theta\le 3\pi/2,\\ \cos((\pi/2-\nu)\epsilon)\cdot\cos((\theta-3\pi/2-\xi)\epsilon) & \text{if } 3\pi/2\le\theta\le 2\pi,\end{cases}$$

with the constants ϵ,R,ξ and ν satisfying the nonlinear relations in [11,22]. Here we choose

$$\epsilon=0.1,\quad \nu=\pi/4,\quad \xi=-14.9225565104455152,\quad R=161.4476387975881,$$

and then the exact solution $u\in H^{1+\epsilon}$ with a singularity at the origin.

We start with a uniform initial mesh $\mathcal{T}_0$ consisting of 128 right triangles and adopt bulk marking strategy by [16] with $\theta=0.2$ as in the previous example. Figure 8(a) plots one adaptive refined mesh and 8(a) plots its corresponding finite element solution. It clearly indicates that recovery type *a posteriori* error estimator (4.18) successfully captures the singularity without introducing any overrefinement. However, the recovery type *a posteriori* error estimator based on classical gradient recovery operators like SPR or PPR have the problem of overrefinement as discussed in [8].

Figure 9(a) shows the numerical errors. One can observe the optimal convergence rate $\mathcal{O}(N^{0.5})$ for energy error and $\mathcal{O}(N^{0.58})$ superconvergence rate for recovered energy error. Figure 9(b) gives the history of effective index. Due to the extreme low global regularity of exact solution, the recovery type *a posteriori* error estimator (4.18) is not asymptotically exact. However, it serves as a robust *a posteriori* error estimator for interface problem as illustrated in Figure 8(a).

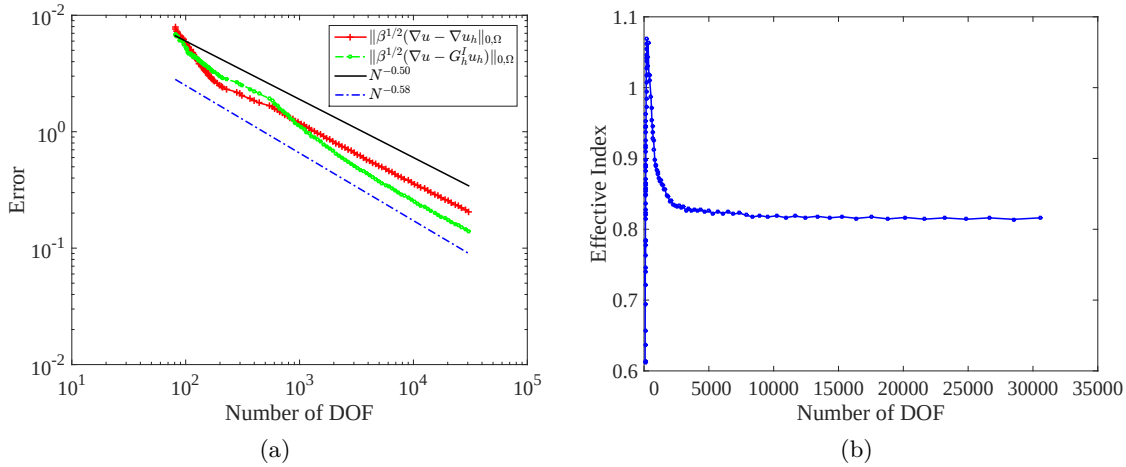

Figure 9: Convergence rates for Example 5.3: (a) Errors; (b) Effective index.

6 Conclusion

In this paper, we develop a new gradient recovery method for elliptic interface problem based on the body-fitted mesh. Specifically, we define an improved gradient recovery operator, which overcomes the drawback that classical gradient recovery method fails to produce superconvergence results when the solution lack regularity at the interface. The superconvergence of this method is proved for both mildly unstructured mesh and adaptive mesh. Several two-dimensional numerical examples are given to confirm our theoretical results, and verify the robustness of the method served as *a posteriori* error estimator. As a continuous study of this work, we develop gradient recovery methods based on unfitted mesh for elliptic interface problem add two references on our recent paper.

Acknowledgement

We thank anonymous referees for valuable suggestions and comments. This work was partially supported by the NSF grant DMS-1418936, KI-Net NSF RNMS grant 1107291, and Hellman Family Foundation Faculty Fellowship, UC Santa Barbara.

References

[1] M. Ainsworth and J. T. Oden, *A posteriori error estimation in finite element analysis*, Pure and Applied Mathematics (New York), Wiley-Interscience [John Wiley & Sons], New York, 2000. MR 1885308

[2] I. Babuška, *The finite element method for elliptic equations with discontinuous coefficients*, Computing (Arch. Elektron. Rechnen) **5** (1970), 207–213. MR 0277119

[3] I. Babuška and T. Strouboulis, *The finite element method and its reliability*, Numerical Mathematics and Scientific Computation, Oxford University Press, New York, 2001. MR 1857191
[4] C. Bernardi and R. Verfürth, *Adaptive finite element methods for elliptic equations with non-smooth coefficients*, Numer. Math. **85** (2000), no. 4, 579–608. MR 1771781
[5] C. Börgers, *A triangulation algorithm for fast elliptic solvers based on domain imbedding*, SIAM J. Numer. Anal. **27** (1990), no. 5, 1187–1196. MR 1061125
[6] J. H. Bramble and J. T. King, *A finite element method for interface problems in domains with smooth boundaries and interfaces*, Adv. Comput. Math. **6** (1996), no. 2, 109–138 (1997). MR 1431789
[7] S. C. Brenner and L. R. Scott, *The mathematical theory of finite element methods*, third ed., Texts in Applied Mathematics, vol. 15, Springer, New York, 2008. MR 2373954
[8] Z. Cai and S. Zhang, *Recovery-based error estimator for interface problems: conforming linear elements*, SIAM J. Numer. Anal. **47** (2009), no. 3, 2132–2156. MR 2519597
[9] C. Chen, *Structure theory of superconvergence of finite elements (in Chinese)*, Hunan Science and Technique Press, Changsha, 2001.
[10] L. Chen and J. Xu, *A posteriori error estimator by post-processing*, Adaptive Computations: Theory and Algorithms (Jinchao Xu and Tao Tang, eds.), Science Press, Beijing, 2007, pp. 34–67.
[11] Z. Chen and S. Dai, *On the efficiency of adaptive finite element methods for elliptic problems with discontinuous coefficients*, SIAM J. Sci. Comput. **24** (2002), no. 2, 443–462 (electronic). MR 1951050
[12] Z. Chen and J. Zou, *Finite element methods and their convergence for elliptic and parabolic interface problems*, Numer. Math. **79** (1998), no. 2, 175–202. MR 1622502
[13] S. H. Chou, *An immersed linear finite element method with interface flux capturing recovery*, Discrete Contin. Dyn. Syst. Ser. B **17** (2012), no. 7, 2343–2357. MR 2946307
[14] S. H. Chou and C. Attanayake, *Flux recovery and superconvergence of quadratic immersed interface finite elements*, Int. J. Numer. Anal. Model. **14** (2017), no. 1, 88–102.
[15] P. G. Ciarlet, *The finite element method for elliptic problems*, Classics in Applied Mathematics, vol. 40, Society for Industrial and Applied Mathematics (SIAM), Philadelphia, PA, 2002, Reprint of the 1978 original [North-Holland, Amsterdam; MR0520174 (58 #25001)]. MR 1930132
[16] W. Dörfler, *A convergent adaptive algorithm for Poisson's equation*, SIAM J. Numer. Anal. **33** (1996), no. 3, 1106–1124. MR 1393904
[17] S. Du, R. Lin, and Z. Zhang, *A posteriori error analysis of multipoint flux mixed finite element methods for interface problems*, Adv. Comput. Math. **42** (2016), no. 4, 921–945. MR 3533521
[18] L. C. Evans, *Partial differential equations*, second ed., Graduate Studies in Mathematics, vol. 19, American Mathematical Society, Providence, RI, 2010. MR 2597943
[19] H. Guo and X. Yang, *Polynomial preserving recovery for high frequency wave propagation*, J. Sci. Comput. (2016), 1–21.
[20] S. Hou and X. D. Liu, *A numerical method for solving variable coefficient elliptic equation with interfaces*, J. Comput. Phys. **202** (2005), no. 2, 411–445. MR 2145387
[21] T. Y. Hou, X. H. Wu, and Y. Zhang, *Removing the cell resonance error in the multiscale finite element method via a Petrov-Galerkin formulation*, Commun. Math. Sci. **2** (2004), no. 2, 185–205. MR 2119937
[22] R. B. Kellogg, *On the Poisson equation with intersecting interfaces*, Applicable Anal. **4** (1974/75), 101–129, Collection of articles dedicated to Nikolai Ivanovich Muskhelishvili. MR 0393815

[23] M. Křížek, H. G. Roos, and W. Chen, *Two-sided bounds of the discretization error for finite elements*, ESAIM Math. Model. Numer. Anal. **45** (2011), no. 5, 915–924. MR 2817550
[24] R. J. LeVeque and Z. Li, *The immersed interface method for elliptic equations with discontinuous coefficients and singular sources*, SIAM J. Numer. Anal. **31** (1994), no. 4, 1019–1044. MR 1286215
[25] Z. Li, *The immersed interface method using a finite element formulation*, Appl. Numer. Math. **27** (1998), no. 3, 253–267. MR 1634348
[26] Z. Li and K. Ito, *The immersed interface method*, Frontiers in Applied Mathematics, vol. 33, Society for Industrial and Applied Mathematics (SIAM), Philadelphia, PA, 2006, Numerical solutions of PDEs involving interfaces and irregular domains. MR 2242805
[27] Z. Li, T. Lin, Y. Lin, and R. C. Rogers, *An immersed finite element space and its approximation capability*, Numer. Methods Partial Differential Equations **20** (2004), no. 3, 338–367. MR 2046521
[28] Z. Li, T. Lin, and X. H. Wu, *New Cartesian grid methods for interface problems using the finite element formulation*, Numer. Math. **96** (2003), no. 1, 61–98. MR 2018791
[29] Q. Lin, H. Xie, and J. Xu, *Lower bounds of the discretization error for piecewise polynomials*, Math. Comp. **83** (2014), no. 285, 1–13. MR 3120579
[30] P. Morin, R. H. Nochetto, and K. G. Siebert, *Convergence of adaptive finite element methods*, SIAM Rev. **44** (2002), no. 4, 631–658 (electronic) (2003), Revised reprint of "Data oscillation and convergence of adaptive FEM" [SIAM J. Numer. Anal. **3**8 (2000), no. 2, 466–488 (electronic); MR1770058 (2001g:65157)]. MR 1980447
[31] L. Mu, J. Wang, G. Wei, X. Ye, and S. Zhao, *Weak Galerkin methods for second order elliptic interface problems*, J. Comput. Phys. **250** (2013), 106–125. MR 3079527
[32] A. Naga and Z. Zhang, *A posteriori error estimates based on the polynomial preserving recovery*, SIAM J. Numer. Anal. **42** (2004), no. 4, 1780–1800 (electronic). MR 2114301
[33] ———, *The polynomial-preserving recovery for higher order finite element methods in 2D and 3D*, Discrete Contin. Dyn. Syst. Ser. B **5** (2005), no. 3, 769–798. MR 2151732
[34] S. Osher and R. Fedkiw, *Level set methods and dynamic implicit surfaces*, Applied Mathematical Sciences, vol. 153, Springer-Verlag, New York, 2003. MR 1939127
[35] C. S. Peskin, *Numerical analysis of blood flow in the heart*, J. Computational Phys. **25** (1977), no. 3, 220–252. MR 0490027
[36] ———, *The immersed boundary method*, Acta Numer. **11** (2002), 479–517. MR 2009378
[37] J. A. Roĭtberg and Z. G. Šeftel′, *A theorem on homeomorphisms for elliptic systems and its applications*, Mathematics of the USSR-Sbornik **78 (3)** (1969), 439–465.
[38] J. A. Sethian, *Level set methods*, Cambridge Monographs on Applied and Computational Mathematics, vol. 3, Cambridge University Press, Cambridge, 1996, Evolving interfaces in geometry, fluid mechanics, computer vision, and materials science. MR 1409367
[39] L. B. Wahlbin, *Superconvergence in Galerkin finite element methods*, Lecture Notes in Mathematics, vol. 1605, Springer-Verlag, Berlin, 1995. MR 1439050
[40] H. Wei, L. Chen, Y. Huang, and B. Zheng, *Adaptive mesh refinement and superconvergence for two-dimensional interface problems*, SIAM J. Sci. Comput. **36** (2014), no. 4, A1478–A1499. MR 3233939
[41] H. Wu and Z. Zhang, *Can we have superconvergent gradient recovery under adaptive meshes?*, SIAM J. Numer. Anal. **45** (2007), no. 4, 1701–1722. MR 2338406
[42] J. Xu, *Error estimates of the finite element method for the 2nd order elliptic equations with discontinuous coefficients*, J. Xiangtan Univ. **1** (1982), 1–5.
[43] J. Xu and Z. Zhang, *Analysis of recovery type a posteriori error estimators for mildly struc-*

tured grids, Math. Comp. **73** (2004), no. 247, 1139–1152 (electronic). MR 2047081

[44] Z. Zhang and A. Naga, *A new finite element gradient recovery method: superconvergence property*, SIAM J. Sci. Comput. **26** (2005), no. 4, 1192–1213 (electronic). MR 2143481

[45] X. Zheng and J. Lowengrub, *An interface-fitted adaptive mesh method for elliptic problems and its application in free interface problems with surface tension*, Adv. Comput. Math. (2016), 1–33.

[46] Y. C. Zhou and G. W. Wei, *On the fictitious-domain and interpolation formulations of the matched interface and boundary (MIB) method*, J. Comput. Phys. **219** (2006), no. 1, 228–246. MR 2273376

[47] Q. Zhu and Q. Lin, *Superconvergence theory of the finite element method (in Chinese)*, Hunan Science and Technique Press, Changsha, 1989.

[48] O. C. Zienkiewicz and J. Z. Zhu, *The superconvergent patch recovery and a posteriori error estimates. I. The recovery technique*, Internat. J. Numer. Methods Engrg. **33** (1992), no. 7, 1331–1364. MR 1161557

[49] ———, *The superconvergent patch recovery and a posteriori error estimates. II. Error estimates and adaptivity*, Internat. J. Numer. Methods Engrg. **33** (1992), no. 7, 1365–1382. MR 1161558